Specific issues for the use of satellite data for limited area models

Reinhold Hess

Deutscher Wetterdienst (DWD)
Postfach 100465, 63004 Offenbach, Germany
reinhold.hess@dwd.de

ABSTRACT

Limited area models have higher resolution in space and time, simulate smaller scale structures and pose particular requirements on the assimilation scheme in comparison to large scale models. For the use of satellite radiances generally the same approaches are applied, however some specific issues exist e. g. for the specification of the background error covariance matrix within the variational schemes and for the prescription of first guess temperature profiles above model top for radiative transfer computations. Bias correction is considered critical in terms of sample size and representativity; some theoretical studies are provided to cover that field.

These issues are addressed within the scope the Project *Assimilation of Satellite Radiances with 1D-Var and Nudging* that has been found within the Consortium on small scale modeling (COSMO) and aims at assimilating ATOVS, SEVIRI and AIRS/IASI radiances into the COSMO model. An overview of the project is presented and preliminary results are already provided for using radiances from AMSU-A and SEVIRI instruments.

Although discussed within the scope of a certain application, the following discussions are considered in general relevant for other variational methods that assimilate satellite radiances for limited area models.

1 Introduction

Limited area models with resolutions from 14 km down to 2 km and less are designed to simulate smaller scale structures in space and time as e. g. orographically forced precipitation and convection. More sophisticated physical packages are used and there are fewer constraints at small scales as hydrostacy and geostrophy. The resulting forecasts are less smooth and the dependence on initial values and the predictability of simulated phenomena is more limited in general compared to large scale modeling. There is high interest in using asynchronous and high frequent observations (geostationary imaging, radar data), especially over land, where limited area models are mainly located.

The quality of forecasts of limited area models namely depend on the model itself, but also crucially on the given initial and boundary data. The initial values should be always close the observations, however it is also essential that they are consistent with the numerical model in terms of resolution, orography and vertical distribution of temperature and humidity etc. in order to avoid spurious effects of initialisation as spin-up/down or gravitational waves during short range forecasts. A better fit of the analysis to the observations not necessarily assures a better forecast. In general it is more difficult to show forecast improvements with smaller domains using satellite radiances.

The importance of a consistent first guess is demonstrated by Figure 1, where a forecast of a tropical typhoon is simulated with the Hydrostatic Regional Model (HRM) of DWD. The reference forecast uses interpolated values from GME as initial values and as an experiment the HRM is initialised with an analysis of 3D-Var based on own forecasts of HRM as first guess. The forecast based on 3D-Var provides much better results of typhoon track and strength than the reference. However no additional observations were used with 3D-Var for this study, the forecast of HRM is improved only by the use of more consistent initial values which are generated by 3D-Var using HRM forecasts as first guess. Typhoon and other small scale features are better

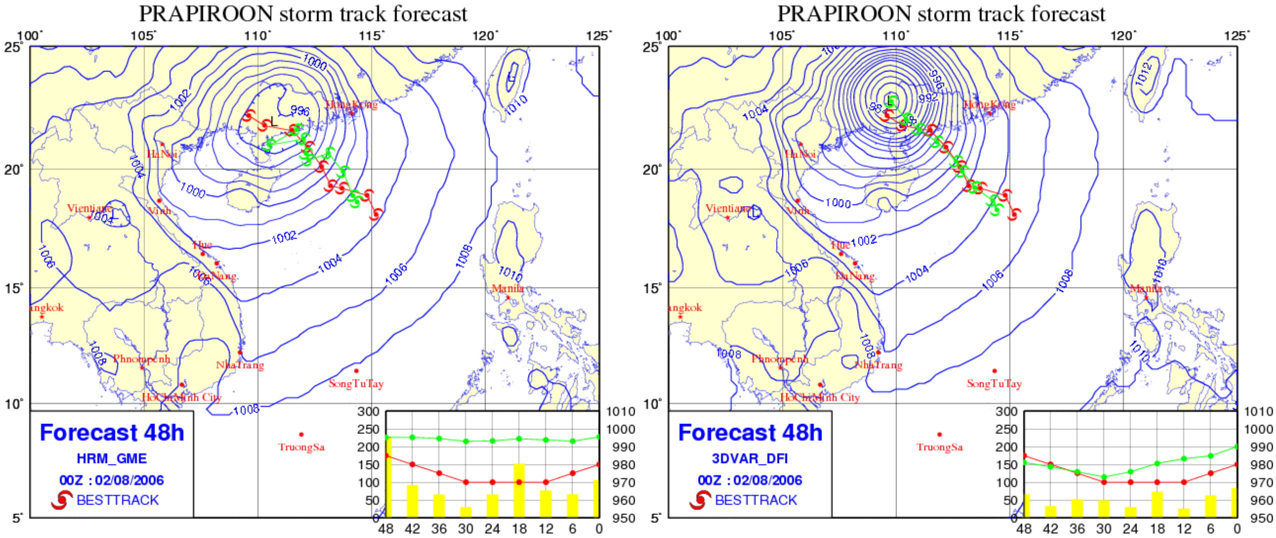

Figure 1: Forecast of HRM (Hydrostatic Regional Model) of DWD based on interpolated values from GME analysis (left) and from 3D-Var analysis that uses HRM forecasts as first guess (right). Resolution of HRM is 14 km, GME values are provided in 60 km grid resolution. At the boundaries forecasts of GME are used in both cases. Courtesy of Le Duc/HMS Vietnam.

represented with the higher resolution of HRM than with the interpolated values from GME.

The configuration of global and limited area models at DWD is presented in Fig. 2 and is an example for a multi-embedded chain of numerical models. The global model GME provides boundary values for COSMO-EU, which itself provides boundaries for COSMO-DE. The domain of COSMO-EU covers large parts over sea, Atlantic Ocean and Mediterranean Sea, and the model is subject to the assimilation of satellite radiances within COSMO therefore.

The COSMO model is applied within the Consortium on small scale modeling in various configurations, an overview of the domains of operational models is presented in Fig. 3 . Other configurations of limited area models exist, Fig. 4 e. g. shows the domains of operational numerical models at Danish Meteorological Institute (DMI). ATOVS radiances are assimilated operationally in the large model with 3D-Var (using FGAT, first guess at appropriate time) with positive impact since 2003 (Amstrup et al. 2003). Radiances are not directly assimilated for the smaller models.

In the following the use of satellite radiances for limited area models is discussed with reference to ATOVS and SEVIRI data within the scope of the Nudging analysis scheme that is enhanced by 1D-Var for satellite radiances. Nevertheless, basic ideas should be relevant for other satellite data as well and in combination with other analysis schemes. Section 2 briefly presents the idea of the Nudging and 1D-Var method, called Nudgevar, which is currently developed at DWD, Section 3 addresses the actual specifics of satellite radiances for limited area models as bias correction, first guess above model top and background errors. Very preliminary results of assimilating ATOVS and SEVIRI data into COSMO-EU are given in Sec. 4 . Conclusions are given in Sec. 5 .

2 Nudging and 1D-Var: Nudgevar

When choosing the assimilation method for limited area models, their specific standards and requirements have to be taken into account. The Newtonian relaxation technique or Nudging Analysis (Stauffer and Seaman 1990) has important characteristics in the context of limited are models and is operationally applied at DWD for the COSMO model since 2000 (formerly LM, Schraff and Hess 2002). Nudging can use straight forward asynchronous observations and deal with any complexity of physics and unsteady solutions, since it does not

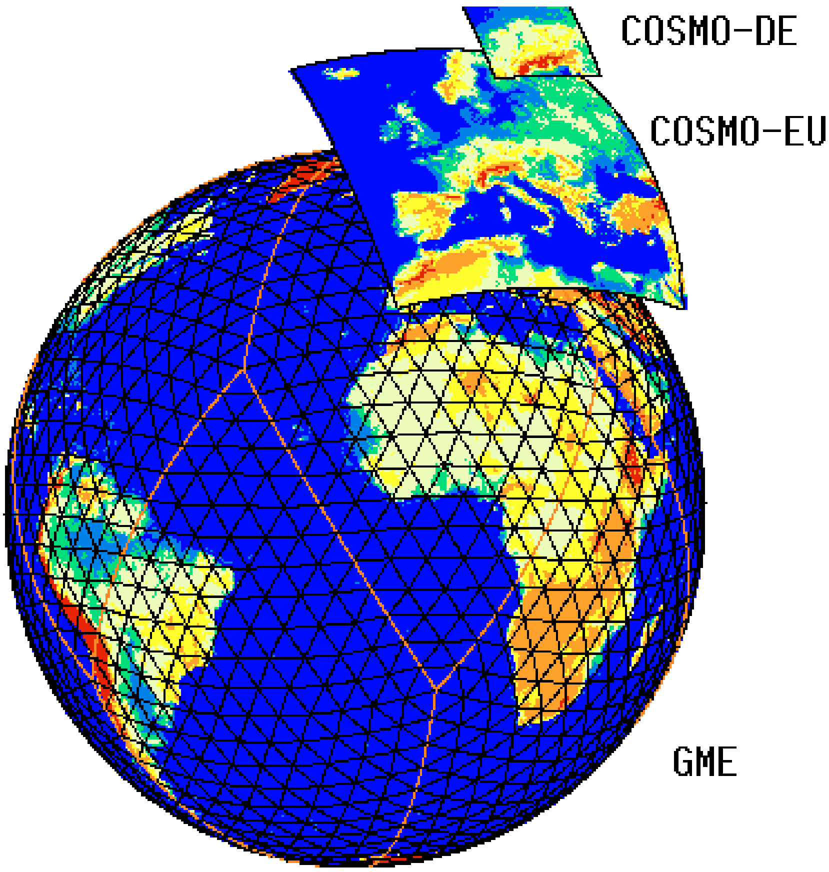

Figure 2: Model configuration at DWD: Local model COSMO-DE gets boundary values from regional model COSMO-EU, which itself is provided by boundaries from global model GME. COSMO-EU is a non-hydrostatic model and discretised on a rotated latitude-longitude grid with mesh size of 7 km and with 40 layers up to 20 hPa. COSMO-DE is based on the same numerical model, but configured with mesh size 2.8 km in order to simulate convection explicitly. Both COSMO models use continuous Nudging for the assimilation of conventional observations and airplane data (and radar reflectivities in case of COSMO-DE). The global model GME is hydrostatic and is discretised on a icosahedral-hexagonal grid with a resolution of 40 km.

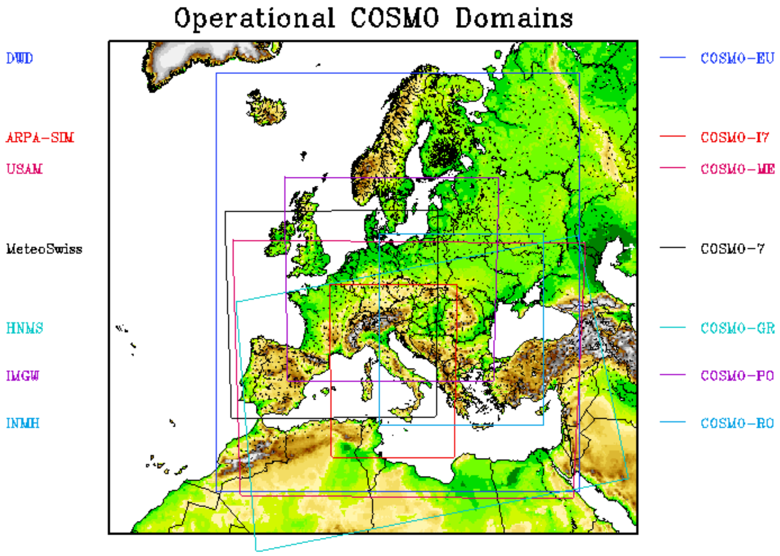

Figure 3: Domains of large operational versions of the COSMO-model including the versions of Germany (DWD: COSMO-EU), Italy (USAM: COSMO-ME and ARPA-SIM: COSMO-I7), Suisse (MeteoSwiss: COSMO-7), Greek (HNMS: COSMO-GR), Poland (IMGW: COSMO-PO), and Rumania (INMH: COSMO-RO). Courtesy of Ulrich Schättler.

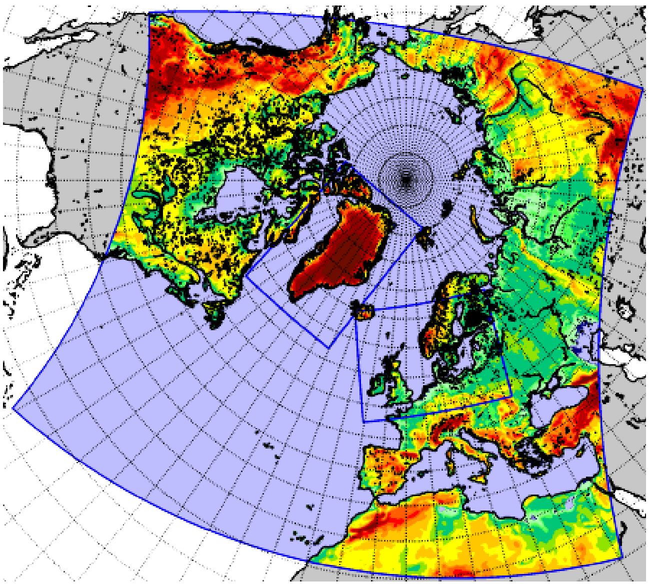

Figure 4: Domains of operational versions of the HIRLAM (HIgh Resolution Limited Area Model) model at DMI (Danish Meteorological Institute). The large model, which covers a considerable part of the northern hemisphere has a grid resolution of about 16 km, the smaller models have grid resolutions of 5 km, all models run with 40 vertical levels. The large model is operated with a 3D-Var analysis system that assimilates ATOVS radiances and is driven with boundary values from IFS of ECMWF. The small models do not have own assimilation systems and are initialised with interpolated values basically from the large model.

require tangent linear or adjoint modules. The computational work is low and initialisation is not required; this allows for timely forecasts which is important for operational short range weather forecasting.

The most prominent backdraw of Nudging is that remote sensing observations with nonlinear observation operators cannot be assimilated directly. In 2005 the COSMO-Project *Assimilation of Satellite Radiances with 1D-Var and Nudging* was found that aims at exploring the use of nonlinear remote sensing data with Nudging in general and specifically at assimilating ATOVS, SEVIRI and also AIRS and IASI data into COSMO-EU and other COSMO models. Profiles of temperature and humidity are derived from the observations using a one dimensional variational method (1D-Var, Chevallier 2001) and are subsequently nudged into the model like conventional observations.

Figure 5 sketches the idea of Nudging: During Nudging Analysis the model trajectory is nudged at every time

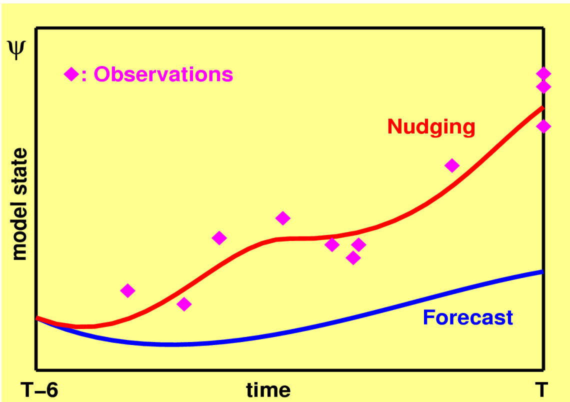

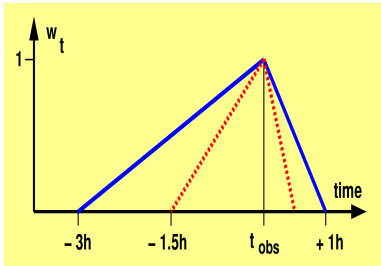

Figure 5: Left: Sketch of Nudging: Any model variable Ψ diverges from the observations during free forecast from time $T-6$ to the time of analysis T. Special nudging terms are added to the model equations that force the model trajectory at each time step during model run towards the observations. The nudged trajectory may follow asynchronous observations with high temporal resolution. Right: The sizes of these additional terms (Nudging weights) depend among others on the difference between observation time and current model time and on the spatial distance of the respective grid point to the observation. Observations are assimilated 1.5 h before and 0.5 h after observation time with a linear increase and decrease of nudging weights (dashed line). Correlations between observations are considered 3 h before and 1 h after observation time (solid line). Courtesy of Christoph Schraff.

step of the forecast model towards the observations with special terms additional to the model equations. The use of satellite observations with 1D-Var requires a first guess which is taken from the current model state of the COSMO-EU. As nudging of a certain observation is started already before its observation time (see Fig. 5), a preliminary 1D-Var retrieval for a temperature and humidity profile is computed with the current available model first guess. This preliminary 1D-Var retrieval is updated at regular intervals with the latest available model first guess until the model time reaches the observation time and the final retrieval can be computed.

For ATOVS data the first retrieval is computed 1.5 h before observation time and is updated every 0.5 h until time of observation. SEVIRI data has a time resolution of only 15 min, the preliminary 1D-Var retrieval is computed 15 min before observation time and the second and final retrieval at observation time; at this time temperature and humidity profile for the next SEVIRI dataset is already retrieved.

The computation of the retrievals with the current available model first guess allows a consistent interaction with conventional observations and other remote sensing data without need for iteration forwards and backwards in time. However, the nudging of the preliminary retrievals leads to correlated errors of satellite radiances and model first guess for later 1D-Var retrievals. The practical implication of this is not clear and have to be taken into account when tuning the background errors and nudging weights.

3 Specific Issues for Limited Area Models in Detail

Satellite radiances can be assimilated into limited area models with variational methods in a very similar way to global models. The assimilation of satellite products of temperature and humidity is not addressed here, these retrievals can be used straight forward as conventional observations. For variational methods however some additional problems and specialties occur for limited area models according to their special application and the resulting design. These special issues comprise the estimation of background errors, bias correction and the definition of the first guess above the model top of the limited area model, which in most cases does not model stratospheric and higher levels that are required for radiative transfer computations.

The mentioned issues are relevant for the use of radiances with 1D-Var and Nudging, but they appear as well in other variational assimilation schemes like 3D-Var and 4D-Var.

3.1 Background Errors

Background errors for high resolution limited area models have less constraints like geostrophy and hydrostacy and should in general prescribe smaller error structures and correlations lengths according to the simulated smaller scales compared to global models. The background error covariance matrix **B** of variational methods is applied as a smoothing operator, that distributes observation increments onto the model grid (for 1D-Var this is done only vertically). With smaller scales and higher variability there is more motivation for situation dependent, flow dependent and adaptive error structures in limited area models.

An example of a situation dependent variability of the background errors is provided in Fig. 6 (Hess 2004). For the global model IFS of ECMWF two test cases were selected that are dominated by persistent and very different weather regimes over central Europe. The background errors of a period with a stable high pressure regime are much smaller and have sharper correlations than those of a period with strong westerly winds.

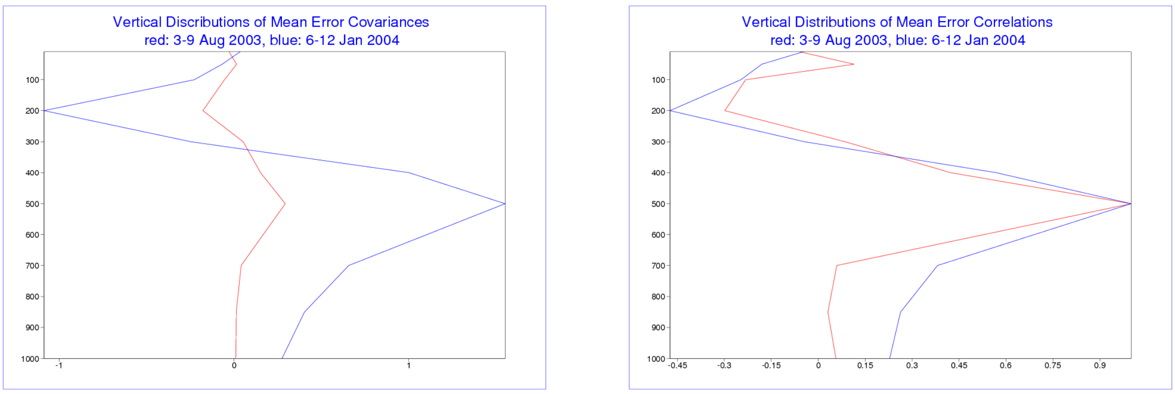

Figure 6: Vertical distributions of mean error covariances and correlations with the 500 hPa level for IFS/ECMWF derived from NMC statistics over central Europe. One test case is 3-9 August 2003 that shows a large high pressure area with low winds and high surface temperatures (red or light lines). The other test case is 6-12 January 2004 with strong westerly winds and lots of rain (blue or dark lines).

The most commonly used method to derive background errors for global models i. e. their variances and covariances, is the NMC-method after Parish and Derber 1992. Forecasts of different length but valid for the same time are compared and their differences are considered estimations of forecast error. The forecasts of limited area models also depend essentially on the provided boundary values and different sets of boundaries result as well in forecast differences. Typically, the shorter forecast of the limited area model is driven by boundary values from the later run of the embedding model. This is consistent with the basic idea of the NMC method and the resulting forecast differences of the limited model are still an estimation for its model error. However, the forecast differences caused by different boundary values may have large scales and dominate the forecast error statistics. When these error statistics are applied to variational methods, 1D-Var (the general conclusion is true also when considering vertical error correlations only), 3D-Var or 4D-Var, the observation is used to correct large scale errors that evolve from the boundaries, and small scale features of the model simulation may be smoothed out.

Siroka et al. 2001 developed the *lagged* NMC method in order to overcome this problem. This variant of the NMC method is similar to the original, but in this case identical boundary values are used for both forecasts. Specifically, the boundary values for the limited area model are provided from the same run of the boundary model. This method actually pretends that the boundaries values are error free and the resulting NMC statistics includes only errors from the differences in the initial values of the forecasts. Consequently the resulting error correlations are much sharper than those derived with the original method.

The assumption of error free boundaries however may be a bit too optimistic, and the background error statistics are sometimes derived with ensemble methods as well, where forecasts with same starting date and forecast length but with perturbed initial state or modified physics are compared (Houtekamer et al. 1996 and Fisher 2003). This method results in error correlations with length scales in between those derived with the standard and the lagged NMC methods.

3.2 Bias Correction

Bias correction is usually applied on the observations; again, the same methods can be used for limited area models as for global methods in general. Potential problems are the size of the statistical samples and the representativity of the results in combination with the choice of predictors. Depending on the location of a limited area model on the globe, a change of seasons and typical weather regimes is experienced with different systematic model errors.

For ATOVS scan line correction and air mass dependent correction are commonly applied (Eyre 1992, Harris and Kelly 2001). SEVIRI data is usually corrected for air mass biases only.

3.2.1 Scan Line Correction

Because of the limited domain size of regional models the data coverage of satellite radiances is small. Longer time series are required in order to obtain sample sizes for statistically significant results, especially for the samples for scan line correction. The required sample size is estimated in the following:

Consider the mean $\mathbf{X} = \frac{1}{n}\sum_{i=1}^{n} x_i$ of random variables $x_{i,i=1,\dots,n}$ with Gaussian distribution, mean m and variance σ_x^2. The variable $\mathbf{X}$ is then Gauss-distributed with mean m and variance $\sigma_{\mathbf{X}}^2$, where

$$\sigma_{\mathbf{X}}^2 = \frac{1}{n^2}\sum_{i=1}^{n}\sigma_x^2 = \frac{\sigma_x^2}{n} \quad . \tag{1}$$

For a demanded error variance $\sigma_{\mathbf{X}}^2$ of $\mathbf{X}$ and given σ_x^2 the required sample size thus is $n \geq \frac{\sigma_x^2}{\sigma_{\mathbf{X}}^2}$. The application of this inequality on observed minus simulated brightness temperatures $x_i = y_i^o - y_i^{fg}$ with standard deviation σ_x leads to an approximation of the required sample size once the maximal acceptable error variance $\sigma_{\mathbf{X}}^2$ is defined. The arbitrarily chosen value $\sigma_{\mathbf{X}}^2$ =(0.01 K)^2 leads to the estimation of required sample sizes as given in Table 1 .

For the COSMO-EU model (domain as in Figs. 2 and 3) two weeks of data are sufficient to achieve the required sample size for each scan line for most relevant sounding channels, whereby data over sea is selected only for bias correction.

Channel	AMSU-A 6	AMSU-A 4	AMSU-A 3
σ_x	0.2 K	0.4 K	1.4 K
n	400	1600	20000

Table 1: Estimation of desired sample sizes n to achieve an accuracy of $\sigma_{\mathbf{X}}$=0.01 K for mean values of observed minus simulated brightness temperatures as computed for bias correction. For selected AMSU-A channels typical standard deviations σ_x of observed minus simulated brightness temperatures are assumed.

Although the size of the sample may be large enough, a selected period of two or more consecutive weeks may not be representative to cover all synoptic scenarios and seasons which are required for stable bias correction. Figure 7 presents scan line biases for the global model GME and for AMSU-A on NOAA-18 for the full domain and for an area similar to that of COSMO-EU. Channels 4 to 12 show very similar results, which suggests that scan line biases do not significantly depend on special synoptic or seasonal situations. These are all included in the global dataset, but not in the sample of the selected area. Particularly there is apparently no latitude dependency on scan line errors for GME. Differences occur for the window channels, where the sampling size is too small to have an accurate estimations of the biases, and for the very high peaking channels, which probably may be caused from an insufficient representativity of the stratosphere. Figure 16 in the Appendix confirms the results for NOAA-16. The scan line biases show very irregular shapes in general, especially Channel 9 of

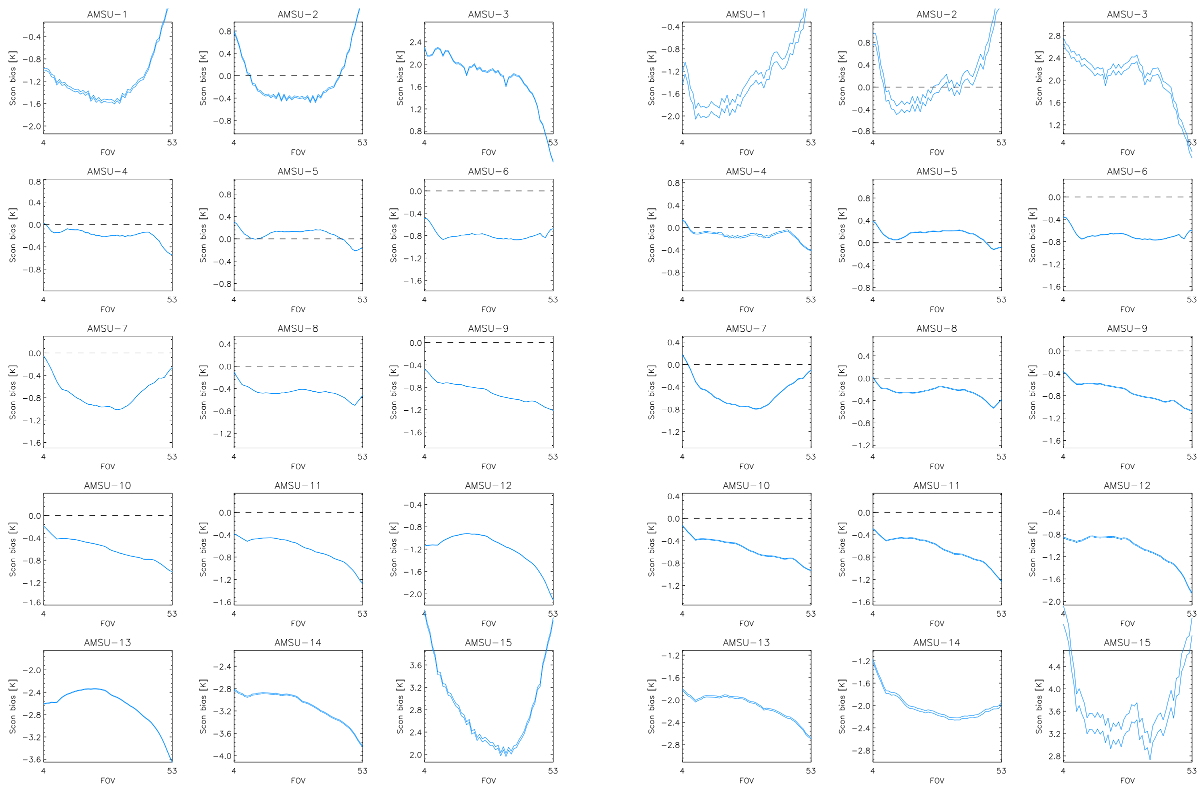

Figure 7: Differences between observed and simulated brightness temperatures for AMSU-A channels 1 to 15 for NOAA-18 (15 to 25 June 2007) for global model GME of DWD by scan line (scan line biases). AMSU-A data has been interpolated to HIRS grid via AAPP. Displayed is mean difference plus/minus standard deviation ($m \pm \sigma_{\mathbf{X}}$, see Eq. (1)). Left: full domain of GME, sample size: 50000 observations per scanline, right: area from latitude 30^o to 60^o and longitude -30^o to 0^o, 1500 observations per scanline (data over sea only in both cases).

NOAA-16 has a very special pattern, which is however statistically significant after considerations above.

A comparison of scan line biases of GME and COSMO-EU is presented in Fig. 8. The scan line biases for

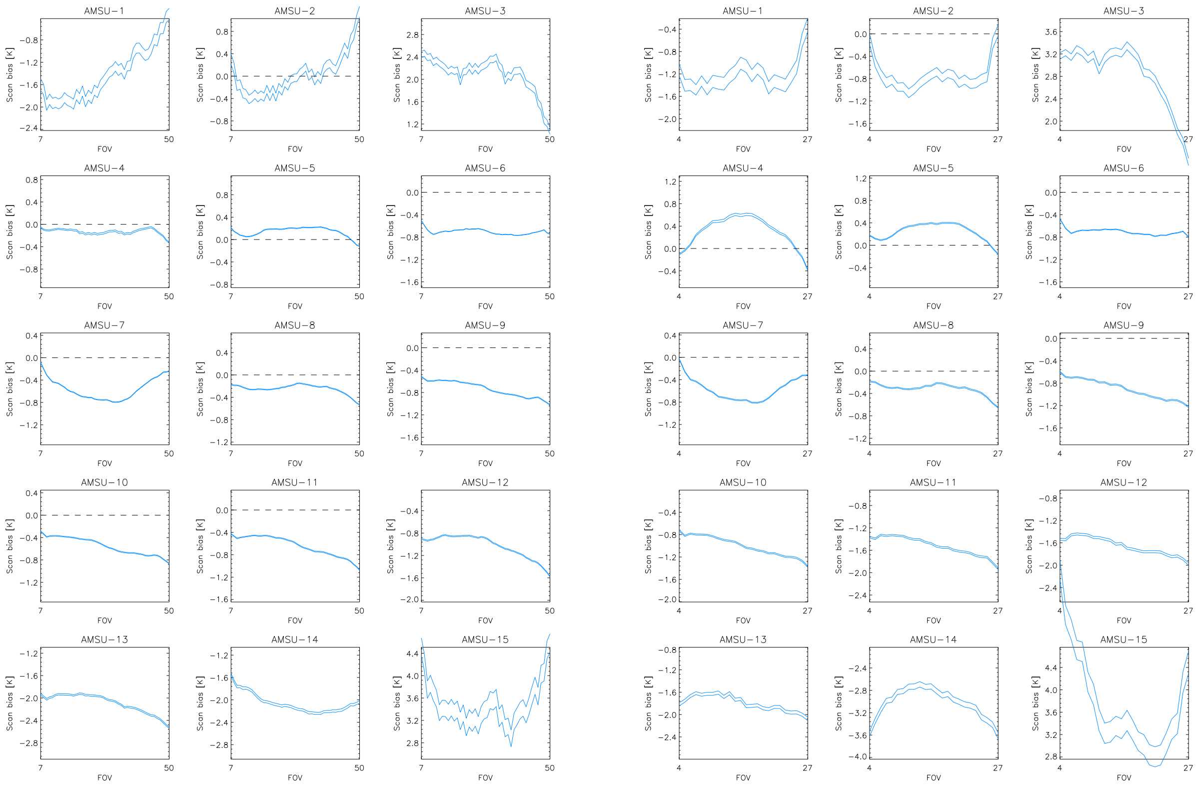

Figure 8: Similar to Fig. 7. Left: GME statistics for area from latitude 30^o to 60^o and longitude -30^o to 0^o, right: statistics for COSMO-EU, approx. 1000 to 1500 observations per scanline. AMSU-A data had been interpolated on HIRS grid for GME statistics, the original instrument grid is used for COSMO-EU. For better visual comparison the outer scanlines are left out in both cases so that beginning and ending of the displayed scanlines coincide.

both models are again very similar for Channels 5 to 12, which is consistent with previous conclusions based on Fig. 7 and suggests, that the scan line biases do neither depend on the synoptic or seasonal situation nor on the specific model (at least not for the two models in question) and that the defined samples are representative for these channels. The central scanlines of Channel 4 show a warmer bias for the COSMO-EU model than for the GME (also slightly for Channel 5). The reason for that is not clear and needs further investigation, since the areas of both models are very similar and the same sea surface temperatures are used in both cases.

3.2.2 Air Mass Correction

The residual bias after scan line correction is considered to be related to the state of the atmosphere and is corrected by air mass bias correction using meteorological predictors. Used sets of predictors are

- observed or simulated brightness temperatures of Channels AMSU-A 4 and 9 or 5 and 9 plus a constant
- mean temperatures (e. g. between 50-200 hPa and 300-1000 hPa), sea surface temperature and integrated water vapour plus a constant
- additionally zenith angle and square of zenith angle (i. e. scan line correction is carried out together with air mass correction, in this case there is no scan line correction in a previous step)

The air mass correction reads $y_i^c = y_i^o - s - c_1\, p_{1,i} - c_2\, p_{2,i} - c_3$ with observations y_i^o and their bias corrected correspondences y_i^c for an example with two predictors $p_{1,i}$ and $p_{2,i}$ plus a constant ($i = 1, \ldots, n$). The parameter s denotes the scan line correction which is often applied before air mass correction. The coefficients c_1, c_2 and c_3 of the linear regression minimise the cost function F

$$F(c_1, c_2, c_3) = \frac{1}{2} \sum_{i=1}^{n} \left(y_i^o - y_i^{fg} - s - c_1\, p_{1,i} - c_2\, p_{2,i} - c_3 \right)^2 \stackrel{!}{=} \min \quad , \tag{2}$$

and can be derived from $\frac{\partial F}{\partial c_1} = \frac{\partial F}{\partial c_2} = \frac{\partial F}{\partial c_2} = 0$. Sometimes different sets of coefficients are used for different latitude bands, however this is apparently neither required for COSMO-EU nor for GME.

Sometimes it is experienced, that only slight changes in the underlying samples e. g. by adding some additional datasets lead to extensive variations in the bias correction coefficients, whereas the applied bias corrections are almost unchanged. This awkward situation is clarified in the following using a Gaussian error analysis, which as well allows to review the choice of predictors and the sample size n that is required to compute stable coefficients.

The coefficients c_1, c_2 and c_3 can be considered functions of the first guess statistics $\Delta y_i = y_i^o - y_i^{fg} - s$ of any specific channel as they are linked by virtue of the cost function F in Eq. (2). After scan line bias correction or simple flat correction with a constant s the first guess statistics Δy_i can be considered bias free, only conditional biases for specific atmospherical states that are defined by the chosen predictors are subject to air mass correction. The gradients of $\nabla_{\Delta y} c_1, \nabla_{\Delta y} c_2$ and $\nabla_{\Delta y} c_3$ with respect to $\Delta y = (\Delta y_{i,i=1,\ldots,n})^T$ are given analytically by the chain rule for implicit functions. The i-th component of the gradients is given as

$$\begin{pmatrix} \frac{\partial c_1}{\partial \Delta y_i} \\ \frac{\partial c_2}{\partial \Delta y_i} \\ \frac{\partial c_3}{\partial \Delta y_i} \end{pmatrix} = -(\nabla^2 F)^{-1} \begin{pmatrix} \frac{\partial^2 F}{\partial c_1\, \partial \Delta y_i} \\ \frac{\partial^2 F}{\partial c_2\, \partial \Delta y_i} \\ \frac{\partial^2 F}{\partial c_3\, \partial \Delta y_i} \end{pmatrix} = -(\nabla^2 F)^{-1} \begin{pmatrix} -p_{1,i} \\ -p_{2,i} \\ -1 \end{pmatrix} \tag{3}$$

with

$$\nabla^2 F = \begin{pmatrix} \sum p_{1,i}^2 & \sum p_{1,i} p_{2,i} & \sum p_{1,i} \\ \sum p_{1,i} p_{2,i} & \sum p_{2,i}^2 & \sum p_{2,i} \\ \sum p_{1,i} & \sum p_{2,i} & n \end{pmatrix} \quad .$$

(the latter summations are from $i = 1$ to n.)

Given the derivatives of the coefficients, linear approximations of the errors Δc_1, Δc_2 respectively Δc_3 of the coefficients can be defined as

$$\begin{pmatrix} \Delta c_1 \\ \Delta c_2 \\ \Delta c_3 \end{pmatrix} = \begin{pmatrix} \nabla_{\Delta y} c_1 \\ \nabla_{\Delta y} c_2 \\ \nabla_{\Delta y} c_3 \end{pmatrix} \Delta y \quad . \tag{4}$$

These errors are unbiased, since the first guess statistics Δy is bias free as well. Finally, the error covariance matrix of the coefficients can be written as

$$\operatorname{cov} \begin{pmatrix} \Delta c_1 \\ \Delta c_2 \\ \Delta c_3 \end{pmatrix} = \begin{pmatrix} \nabla_{\Delta y} c_1 \\ \nabla_{\Delta y} c_2 \\ \nabla_{\Delta y} c_3 \end{pmatrix} \operatorname{cov}\big(\Delta y\big) \Big(\nabla_{\Delta y} c_1, \nabla_{\Delta y} c_2, \nabla_{\Delta y} c_3 \Big) = (\nabla^2 F)^{-1}\, \sigma_x^2 \quad , \tag{5}$$

using $\operatorname{cov}\big(\Delta y\big) = \mathbf{I}_n\, \sigma_x^2$, where $\mathbf{I}_n$ is the identity matrix of order n and σ_x^2 the standard deviation of $\Delta y_{i,i=1,\ldots,n}$ (assuming that the observation increments $\Delta y_{i,i=1,\ldots,n}$ are not correlated).

Equation (5) gives the estimated error variances of the coefficients c_1, c_2 and c_3 and, furthermore, also the covariances and correlations between their errors. Note, that Hessian ∇^2 and error correlation matrix only depend on the values of the predictors and is the same for all channels (when applied in the same way for all channels).

Exemplary Gaussian error analyses have been performed for the predictors AMSU-A 4 and 9 (and a constant); the resulting error correlation matrices are shown in Table 2 . The estimated errors appear to be highly correlated, extremely high for COSMO-EU, but also very strong correlations exist for GME with statistics based on the limited area. For the GME with full statistics the correlations are weaker, but still high, e. g. the constant and Channel 4 are (anti)correlated by -0.91. These high correlations cause the high variations of the bias correction

$$\text{COSMO-EU:} \qquad \text{cor} = \begin{pmatrix} 1.00 & 0.94 & -0.99 \\ 0.94 & 1.00 & -0.98 \\ -0.99 & -0.98 & 1.00 \end{pmatrix}$$

$$\text{GME (lim. area):} \qquad \text{cor} = \begin{pmatrix} 1.00 & 0.88 & -0.98 \\ 0.88 & 1.00 & -0.95 \\ -0.98 & -0.95 & 1.00 \end{pmatrix}$$

$$\text{GME (full domain):} \qquad \text{cor} = \begin{pmatrix} 1.00 & 0.60 & -0.91 \\ 0.60 & 1.00 & -0.87 \\ -0.91 & -0.87 & 1.00 \end{pmatrix}$$

Table 2: Estimated error correlations matrices of bias correction coefficients c_1, c_2 and c_3 for COSMO-EU, GME (area from latitude 30º to 60º and longitude -30º to 0º) and GME (full domain). Correlations derived according to Eq. (5) for observed channels AMSU-A 4 and 9 and a constant as predictors. The first guess statistics are selected over sea only for time period 15 to 25 June 2007.

coefficients. At first glance the correlations are not harmful since the variations of the coefficients cancel out and lead to almost unchanged bias corrections. However, overfitting may be caused, which is useless, if noise is fitted, or corruptive, if signal is fitted and removed. One way to solve this problem is to review the choice of predictors (in the given example at least one predictor should be removed). It is more favourable, however, to gather representative statistics that comprise all atmospheric states that cause systematic changes in the first guess statistics. Ideally, the predictors should be chosen to model the biases that are caused by errors of instruments and radiative transfer computation in dependence on air mass. The presented Gaussian error analysis may support the choice of predictors and the selection of representative meteorological cases.

Sometimes long time series of several months are used for sampling the bias correction statistics, however this may cause problems for limited area models that experience different seasons that cause trends in biases.

After bias correction the first guess statistics look like Figure 9 that shows time series bias corrected observations minus first guess for NOAA-18 and COSMO-EU. Channel 4 has comparatively large standard deviations due to surface emissivity, Channels 5 to 7 show very small and stable biases and deviations. However there are large variations in the biases for the higher peaking Channels 8 to 11; these variations will be addressed in Section 3.3 . Similar results are obtained for NOAA-16, as shown in Fig. 18 in the Appendix.

3.3 First Guess above Model Top

The simulation of satellite radiances for variational analysis schemes requires first guess profiles of temperature and humidity. For stratospheric and, because of the broad weighting functions, also for higher tropospheric sounding channels reasonable first guess values are required high up in the stratosphere and above. The model top of limited area models is usually not high enough to provide these values[1].

For the current application of COSMO-EU profiles of ERA-40 (Uppala et al. 2005) are used as first guess values above 30 hPa.

Figures 9 and 18 show variability of the biases in time that increase for Channels 8 to 11 with the heights of sensitivity of the channels. This variability occur due to inaccurate first guess values in upper levels, that do not capture observed meteorological changes. To some extent this may be caused by an inaccurate model top

[1] For COSMO-EU the model top is 30 hPa, for the HIRLAM model 10 hPa and for the ALADIN model 1 hPa (at least in some model configurations). However, the commonly used fast radiative transfer model RTTOV (Sounders et al. 1999) requires temperature profiles up to 0.1 hPa or even 0.05 hPa in order to simulate all channels of the available instruments.

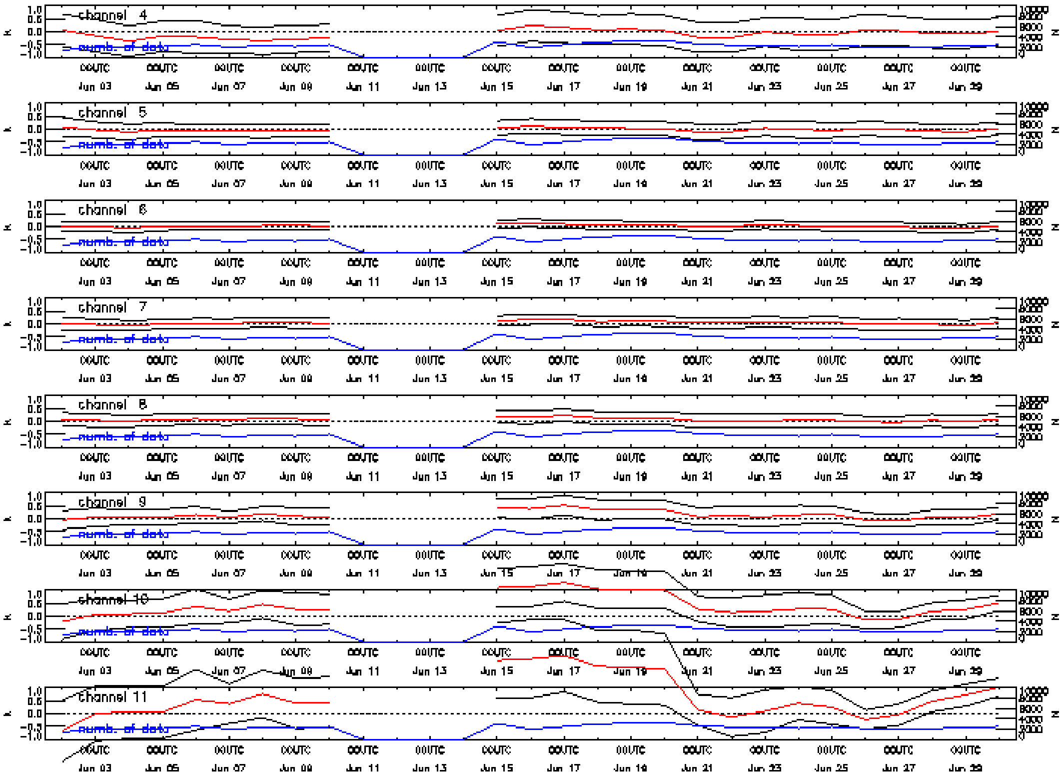

Figure 9: Time series of differences between bias corrected observations and first guess simulations for AMSU-A Channels 4 to 11 on NOAA-18 based on COSMO-EU. Displayed is mean, mean plus/minus standard deviation and number of data. For bias correction all data available in June 2007 were used (which shows already slightly weaker error correlations of the coefficients than these given in Table 2).

of COSMO-EU but a comparison to channel sensitivity reveals that they are mainly consequence of the use of climatological values above 30 hPa that do not follow topical stratospheric conditions. This high variability of the biases prevents the assimilation of these channels with optimal impact. Several options are available to prescribe the required first guess above model top:

- Climatological values may be used as currently applied and discussed for COSMO-EU, probably in combination with the next item.
- Only the lower peaking channels are used that are not affected too much by inaccurate first guess values in the troposphere and above. The low peaking channels are most important especially for limited are models, as they contain most relevant information for the lower troposphere.
- The model top may be increased to the required height. However, this requires good model analyses and forecasts in the stratosphere (with high wind speeds that may limit time stepping) in order to provide reasonable values at the top levels as well.
- First guess values of another higher peaking model may be used above model top, most conveniently of the model that already provides the boundary values[2].
- The stratospheric first guess may be retrieved with high peaking channels that are not directly assimilated in order to support the assimilation of the remaining lower peaking channels (Barwell 1996).

The last option had been operational at the Met. Office (UK) for some time and is discussed here in more detail: The first guess profile of temperature x may be retrieved with high sounding channels y using a linear regression

$$s = \mathbf{W} y \quad , \tag{6}$$

where $\mathbf{W}$ is the regression matrix that is derived using a training data set containing representative samples of pairs of x and y. This simple linear regression (6) is reasonable, since the relation between temperature and temperature sounding channels is almost linear in high stratosphere as humidity and clouds are not relevant. Figure 10 shows scatterplots of linearly retrieved temperatures against an independent dataset of temperature profiles from IFS. The errors are very large for the top levels, but they decrease essentially for the lower peaking levels to values about 5 K. However, the accuracy of retrieved profiles may be actually higher, since IFS forecasts may not have detected any stratospheric anomalies correctly (e. g. polar vortex). A drawback of the latter method is its combination with bias correction for the radiances; it may be required to monitor and recompute the regression matrix $\mathbf{W}$ from time to time.

4 Preliminary Results

Very preliminary results are presented in the following for the assimilation of ATOVS and SEVIRI radiances with 1D-Var and Nudging into COSMO-EU. Methods to assimilate microwave data over land are in the stage of development for global models and probably similar approaches can be used for regional models. The same is true for the assimilation of cloudy or rainy radiances in the infrared respectively microwave spectrum. The use of radiances over sea and in case of clouds or precipitation goes beyond the scope of the presented development and this paper; results are shown for radiances free of cloud and precipitation over sea only.

4.1 AMSU-A

Microwave radiance are the backbone satellite observing system for global models and it suggests itself to use them for limited area models, although the data coverage of polar orbiting satellites may be poor. For this study

[2]But also other models may be used: As the global model GME of DWD with a model top of 10 hPa still is not high enough, forecasts of IFS are received timely in order to expand the first guess for the assimilation of radiances for GME.

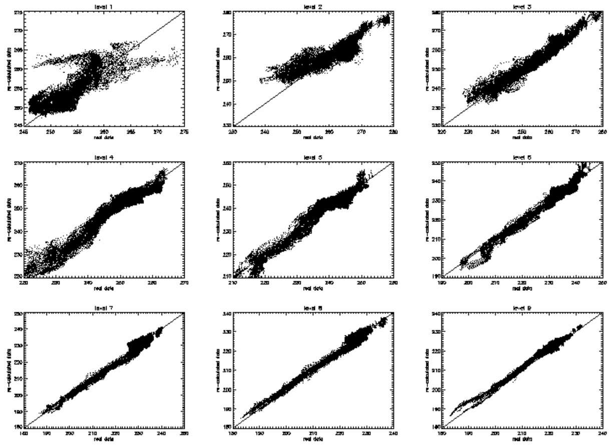

Figure 10: Scatterplots of retrievals according to Eq. (6) against independent validation dataset of IFS forecasts. Regression is performed for top ten levels of RTTOV-7 (i. e. 0.1, 0.29, 0.60, 1.42, 2.611, 4.407, 6.95, 10.37, and 14.81 hPa). Regression matrix **W** *has been computed with temperature profiles of 12 to 33 hourly forecasts of IFS that are operationally used for the assimilation of satellite radiances for the global model GME at DWD.*

the satellites NOAA-15, 16 and 18 are used, that altogether deliver at least some reasonable date coverage for the COSMO-EU within every three hours.

Microwave radiances contaminated by rain are detected by the surface type classification scheme of Kelly and Bauer 2000. Figure 11 gives a validation study over the North Sea, where cloudy and rainy observations are flagged in good agreement with the satellite image from MSG. According to Sec. 3.3 only Channels 5 to 7 of

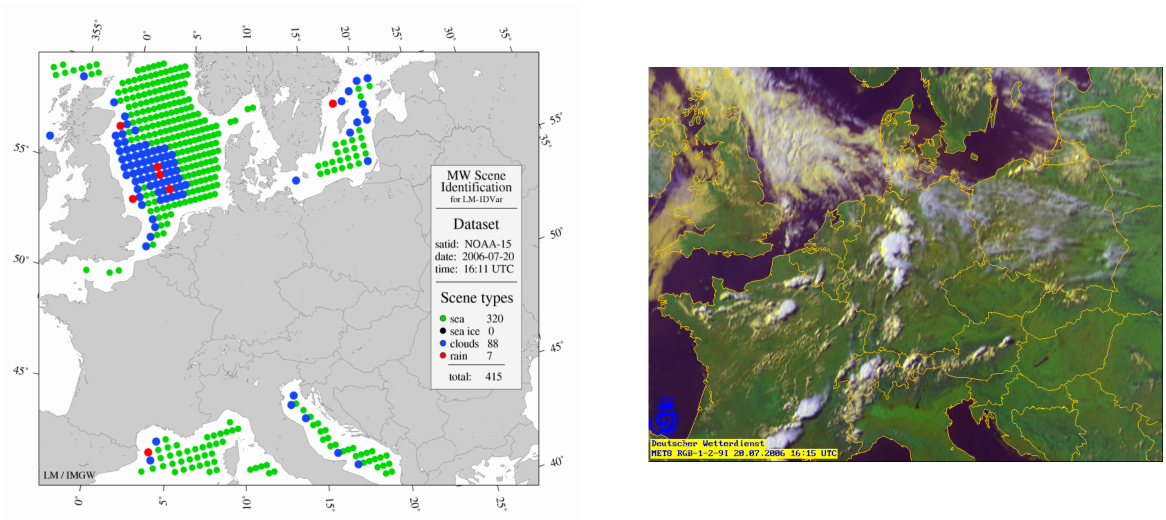

Figure 11: Left: Microwave surface classification. Green: cloud free and thin clouds, blue: thick clouds, red: rain. Right: independent validation with MSG imaging. Courtesy of Blazej Krzeminski.

NOAA-15, 16 and 18 are assimilated (besides the defective Channel 6 of NOAA-15). A trial study of COSMO-EU with 1D-Var for AMSU-A and Nudging is presented in Fig. 12 for 20 March 2007, 0 UTC: The reference forecast shows an overpredicted low over the Baltic Sea with strong wind gusts of over 30 m/s in northern Germany. The low was generated within the model domain of COSMO-EU and is not driven by boundary conditions. Two studies with different thinning options show slightly better results if compared subjectively to the analysis. The improvement is small, however encouraging; more positive impact is expected with a better

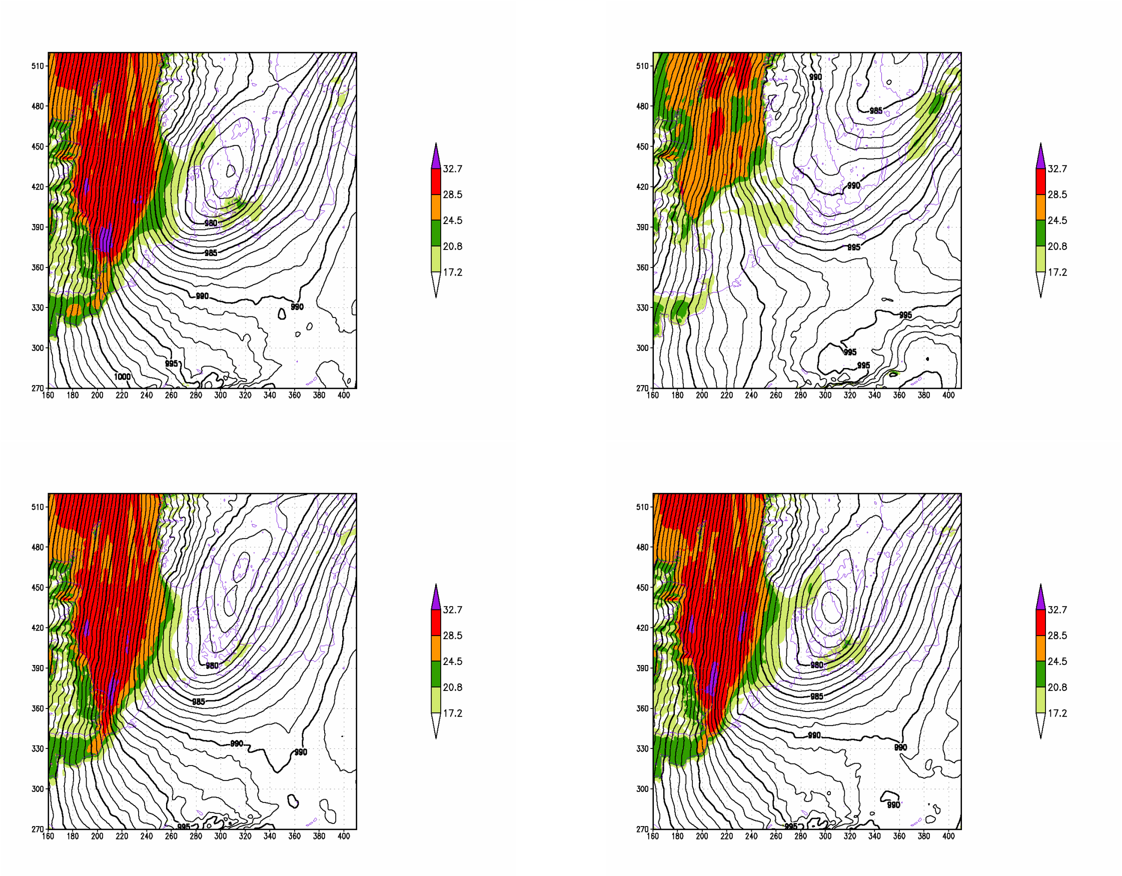

Figure 12: Trial study of COSMO-EU with two different thinning strategies. Displayed is the mean sea level pressure with lines and maximal 10 m wind gusts in shades. Top: Reference forecast (left), verifying analysis (right). Bottom: Trial forecasts with 1D-Var and Nudging. Every second respectively third observation is active after thinning (left and right). Valid date of analysis and forecasts is 20 March 2007, 0 UTC with a forecast length of 48 h.

tuning of the 1D-Var scheme and the nudging coefficients in general. However, this special case may be a model problem as well.

4.2 SEVIRI

The increased number of channels with SEVIRI compared to MVIRI and a very high temporal sampling suggests the assimilation of radiances from the geostationary satellites Meteosat-8 and successors for limited area models. After theoretical studies (e. g. Di Giuseppe et al. 2001) of information content the most important channels for NWP are the two water vapour channels at 6.2 μm and 7.3 μm wavelength. For the first trial runs these water vapour channels are used along with infrared channels at 8.7 μm, 10.9 μm and 12.0 μm over sea and for cloud free observations with a time resolution of 15 min. Cloud detection is performed using the cloud classification product of the NWC-SAF (Derrien and Le Gléau 2005, see Fig. 13); only cloud free observations are assimilated with 1D-Var and Nudging.

The selected case of 8 July 2004 for the assimilation of Meteosat-8 SEVIRI radiances is a false alarm case with large atmospheric instability and strong convection in north of Italy in the reference forecast. The actual event was of much minor intensity, drier winds with scattered thunderstorms appearing only in the early morning

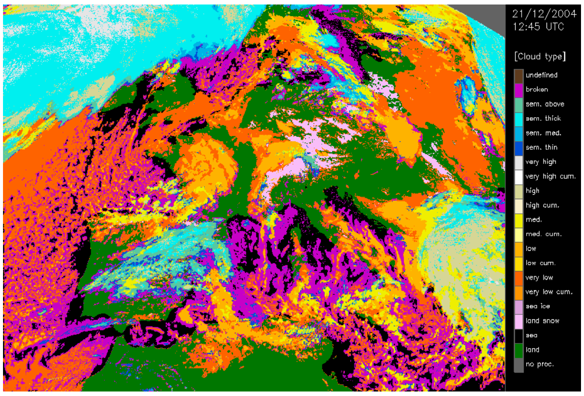

Figure 13: Cloud classification product of Nowcasting (NWC)-SAF, which is used for cloud detection (Derrien and Le Gléau 2005) Only black data is used (cloud free over sea).

of the 9th July, see Fig. 14 (left respectively right). The forecast shows too heavy precipitation compared to

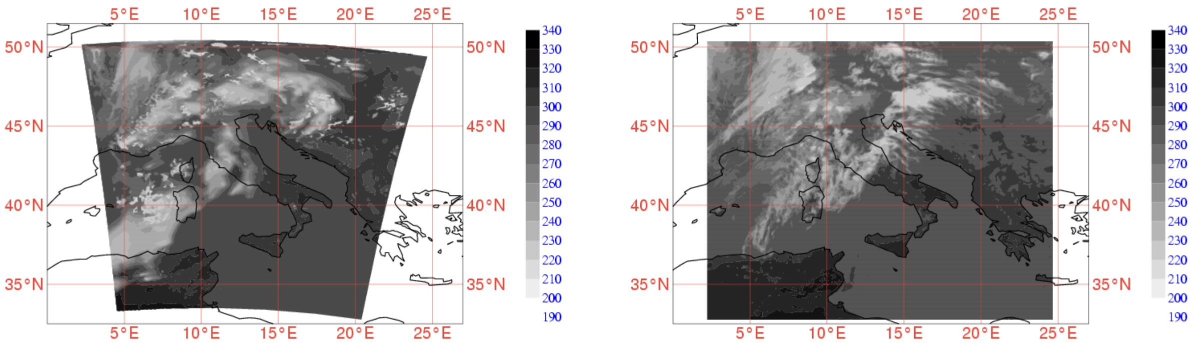

Figure 14: Left: Synthetic satellite image based on reference forecasts of the COSMO model for test case of 8 July 2004. Right: True satellite image of SEVIRI/Meteosat-8 for same date.

observations in large parts of northern Italy as displayed in Fig. 15 . The trial forecasts with assimilation of SEVIRI radiances slightly decrease but still overestimate precipitation in the highlighted areas north east and north west of Italy. Again, more improvement is expected with thorough tuning of 1D-Var error specifications and nudging weights.

5 Conclusion

Resolution of satellite sounding instruments increase in space, time, and also spectrally and provide more and more wealthy information for global and limited area models, where similar approaches can be applied to exploit the data. There is even more interest for highly resolved observations in general for limited area models, especially for high resolution in time. The question arises, which is an optimal analysis scheme, that is able to assimilate the data in combination with highly nonlinear and small scale processes. Side constraints like forecast predictability and dependence on initial and boundary values have to be taken into account.

The Nudging analysis scheme is considered an reasonable approach in this context, moreover, its computation is fast and allows for timely short range weather forecasts.

The main weakness of Nudging is a missing stringent mathematical framework that guarantees a consistent use of observations and optimal solutions after defined assumptions as variational methods have. A combination of

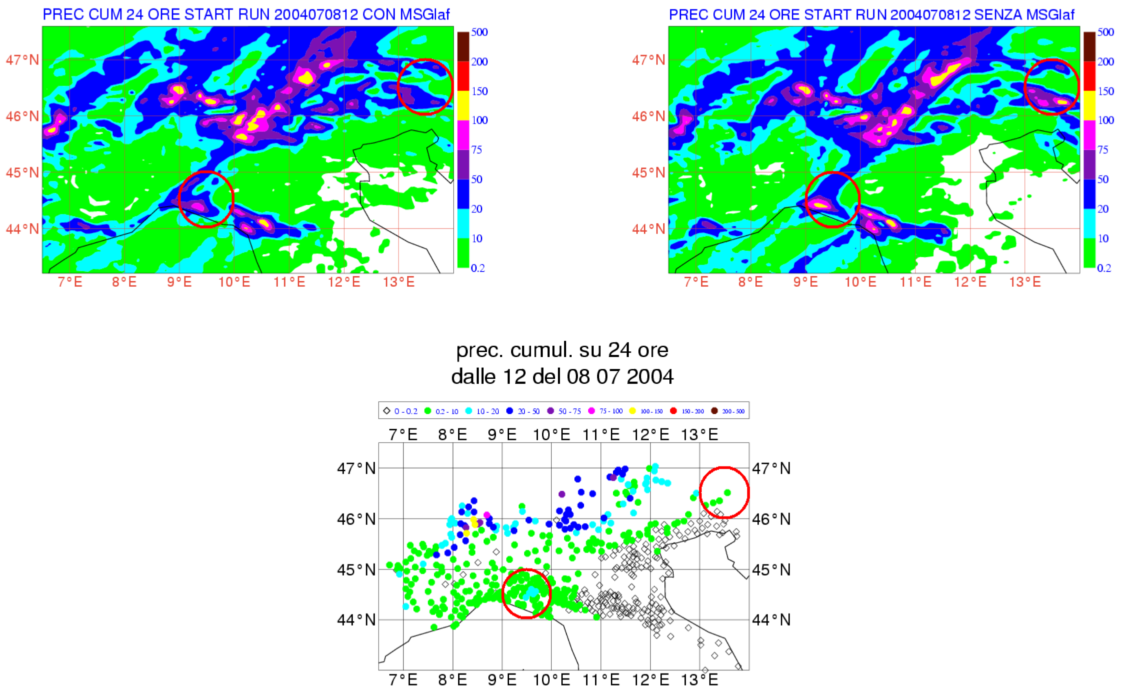

Figure 15: Top: 24 h integrated precipitation of test study with 1D-Var and Nudging of SEVIRI radiances of Meteosat-8 (left) and reference forecast (right). Bottom: observed precipitation. For areas north east and north west of Italy (highlighted by circles) the overestimation of precipitation is slightly reduced by the assimilation of SEVIRI radiances compared to the reference forecast.

Nudging with variational ideas e. g. for the consistent prescription of the nudging weights for the observations could modernise the Nudging approach, as the nudging weights express the mapping of observation increments onto the model grid as the background error covariance matrix **B** does in variational methods.

Some specialties and complications exist when using satellite radiance for limited area models compared to global models. Among them are bias correction, the prescription of temperature profiles above model top for the radiative transfer simulation and the specification of background errors. The latter express errors of the background that include small scale features of the simulation but also errors introduced from the boundaries with much larger error structures. The background error covariance matrix filters the observation increments onto the model grid and ideally creates corrections that are specific to the scale of the current error structure. There are less constraints (hydrostacy, geostrophy) on smaller scales and the interest for adaptive, localised and flow or situation dependent background error increase in general for limited area models. Especially the increased vertical resolution of modern infrared sounders should not be smoothed out by inadequate large background error correlations.

As far as bias correction is concerned, the sample size is not found exceptionally critical, even not for scan line correction of AMSU-A. The required time to gather reasonable samples depend on the size of the model domain (especially over sea). For COSMO-EU about two weeks were found sufficient to provide reliable estimations of the scan line biases for most relevant tropospheric channels. The choice of predictors for the air mass dependent bias correction is more crucial in combination with the representative meteorological situations for which the bias correction coefficients are computed. Longer time series of several months or a sample of selected scenarios are useful to prevent overfitting with highly correlated predictors.

The forecast quality of limited area models depends essentially on boundary values and also on the quality of the forecast models itself including more and more sophisticated physics. In general less improvement can be expected for limited area models when assimilating observations and satellite radiances specifically compared to global models. The verification of limited area models is more demanding as well, much longer statistics are required in order to provide significant results.

Most prominent challenges for the improved assimilation of radiances is to enhance data coverage, i. e. the use of microwave data over land, where most local models are located, and the use of infrared data in case of clouds, as only about 5 % of all infrared data is cloud free. Methods for both applications are currently developed intensively for global models and should be applicable for local area models with very similar approaches in future.

6 Acknowledgments

The development of 1D-Var within Nudging has been performed in the COSMO-Priority Project *Assimilation of Satellite Radiances with 1D-Var and Nudging*. The author thanks the members of the project team for their contributions to the paper: Francesca Di Giuseppe has computed the presented test case for SEVIRI data (Figs. 14 and 15), Christoph Schraff has selected and run tests with AMSU-A (Fig. 12), while Blazej Krzeminski has contributed a lot to the implementation especially for AMSU-A. Thanks also to Bjarne Amstrup for discussions about and results from the HIRLAM model (Fig. 4).

7 References

Amstrup B., 2003: *Impact of NOAA16 and NOAA17 ATOVS AMSU-A radiance data in the DMI-HIRLAM 3D-Var analysis and forecasting system — january and february 2003*. DMI scientific report 03-06, Danish Meteorological Institute.

Barwell B. R., 1996: *Recent advances in satellite sounding at the UK Meteorological Office* International

Geoscience and Remote Sensing Symposium, 1996. IGARSS ’96. Remote Sensing for a Sustainable Future. Volume 3, Issue, 27-31 May 1996 Page(s):1438 - 1440 vol. 3.

Chevallier F., 2000: *A one dimensional variational analysis package*, NWP SAF report NWPSAF-ECUD-001, Jan 2000.

Derrien M. and Le Gléau H., 2005: *MSG/SEVIRI Cloud Mask and Type from SAFNWC*, I. J. R. S., vol. 26, No. 21, pp 4707-4732, DOI: 10.1080/01431160500166128.

Di Giuseppe F., M. Elementi, D. Cesari, and T. Paccagnella: *The potential of variational retrieval of temperature and humidity profiles from Meteosat Second Generation observations*, Q. J. R. Meteorol. Soc., **128**, to appear

Eyre J. R., 1992: *A bias correction scheme for simulated TOVS brightness temperatures*. ECMWF Tech. Memo. 186, 28 pp.

Fisher M., 2003: *Background error covariance modeling. Proceedings of the ECMWF Seminar on Recent developments in data assimilation for atmosphere and ocean*, 8-12 September 2003, 45-63.

Harris B. and G. Kelly, 2001: *A satellite bias correction scheme for radiance assimilation*. Quart. J. Roy. Meteor. Soc., **127**, pp. 1453-1468.

Hess R., 2004: *The specification of background error covariances for radiance assimilation*, EUMETSAT NWP-SAF Visiting Scientist Report.

Houtekamer P. L., L. Levaivre, J. Derome, H. Ritchie, and H. L. Mitchell, 1996: *A system simulation approach to ensemble prediction*. Mon. Wea. Rev., 124, 1225-1242.

Kelly G. and P. Bauer, 2000: *The use of AMSU-A surface channels to obtain surface emissivity over land, snow and ice for Numerical Weather Prediction*, Proc. of the Eleventh International TOVS study conference, Budapest, Hungary, 167-179.

Parish D. F. and J. C. Derber, 1992: *The National Meteorological Center’s spectral statistical interpolation analysis system*, Mon. Weather Rev., 120, 1747-1763.

Saunders R., M. Matricardi, and P. Brunel, 1999: *An improved fast radiative transfer model for assimilation of satellite radiance observations*. Quart. J. Roy. Meteor., 125, 1407-1425.

Saunders R., P. Brunel, F. Chevallier, G. Deblonde, S. J. English, M. Matricardi, and P. Rayer, 2002: *RTTOV-7 science and validation report*, UK Met Office, Met Office Forecasting and Research Technical Report No. 387.

Schraff C. and R. Hess, 2002: *Realisierung der Datenassimilation im LM*, promet, Vol. 27, Heft 3/4.

Siroka M., C. Fischer, V. Casse, R. Brozkova, and J. F. Geleyn, 2001: *The definition of mesoscale selective forecast error covariances for a limited area variational analysis*. Meteor. Atmos. Phys., special issue of the SRNWP Workshop on high-resolution modeling, Offenbach, 25-27 October 1999.

Stauffer D. R. and N. L. Seaman, 1990: *Use of four-dimensional data assimilation in a limited-area mesoscale model. Part I: Experiments with synoptic-scale data*. Mon. Wea. Rev., 118, 1250-1277.

Uppala S. M., P. W. Kallberg, A. J. Simmons, U. Andrae, V. da Costa Bechtold, M. Fiorino, J. K. Gibson, J. Haseler, A. Hernandez, G. A. Kelly, X. Li, K. Onogi, S. Saarinen, N. Sokka, R. P. Allan, E. Andersson, K. Arpe, M. A. Balmaseda, A. C. M. Beljaars, L. van de Berg, J. Bidlot, N. Bormann, S. Caires, F. Chevallier, A. Dethof, M. Dragosavac, M. Fisher, M. Fuentes, S. Hagemann, E. Holm, B. J. Hoskins, L. Isaksen, P. A. E. M. Janssen, R. Jenne, A. P. McNally, J.-F. Mahfouf, J.-J. Morcrette, N. A. Rayner, R. W. Saunders, P. Simon, A. Sterl, K. E. Trenberth, A. Untch, D. Vasiljevic, P. Viterbo, and J. Woollen, 2005: *The ERA-40 re-analysis*. Quart. J. R. Meteorol. Soc., 131, 2961-3012.

8 Appendix

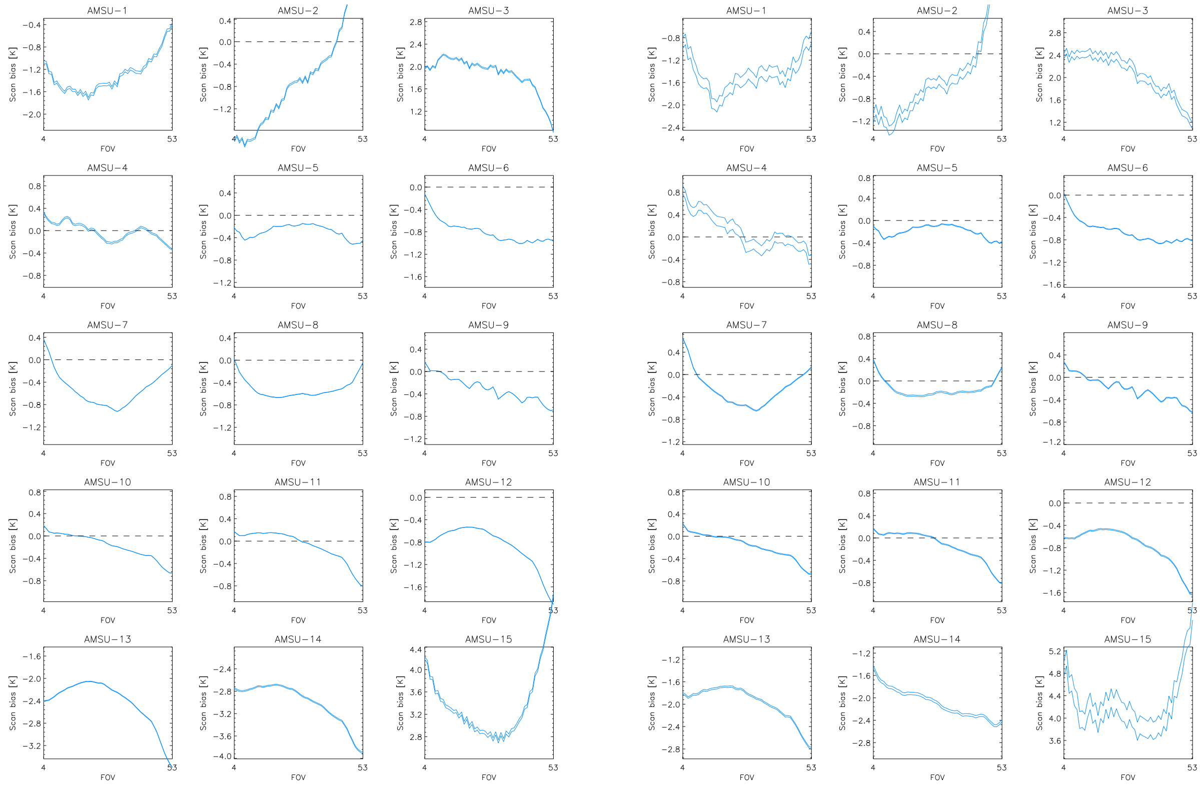

Figure 16: As Fig. 7 but for NOAA-16. Note that Channel 4 of NOAA-16 has increased noise.

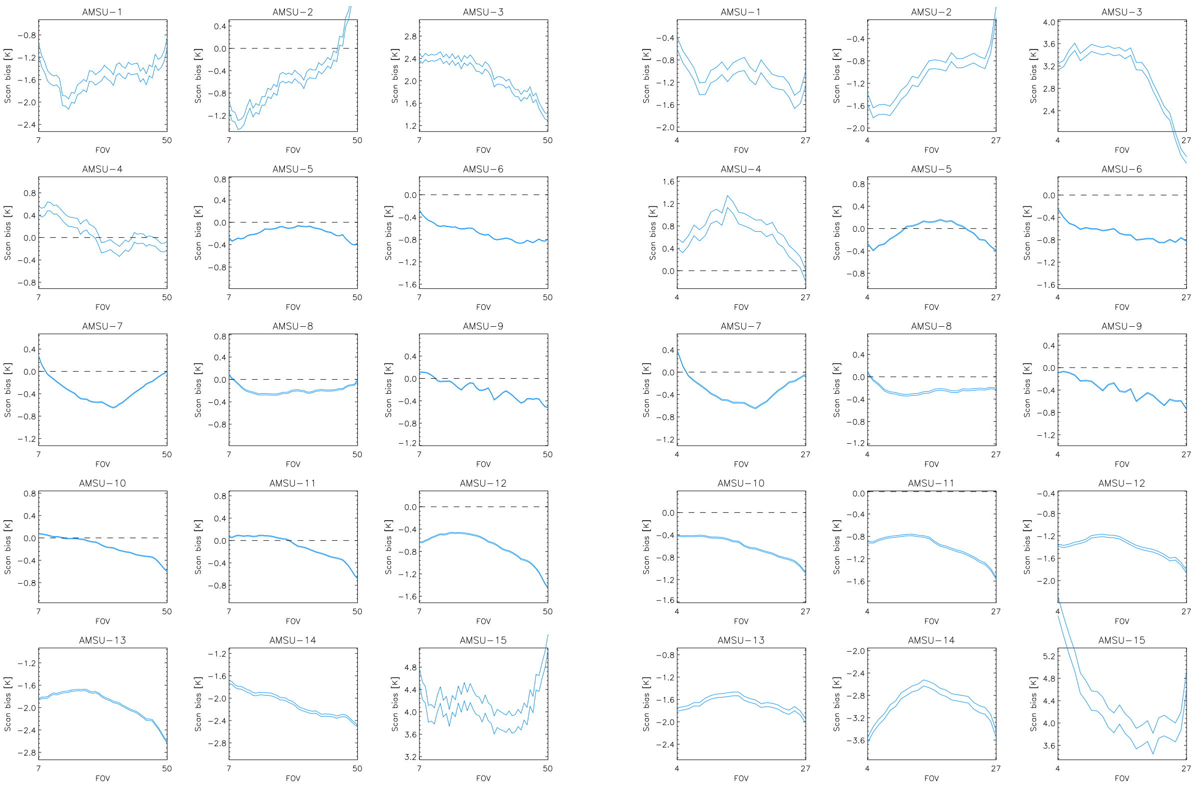

Figure 17: As Fig. 8 but for NOAA-16. Note that Channel 4 of NOAA-16 has increased noise.

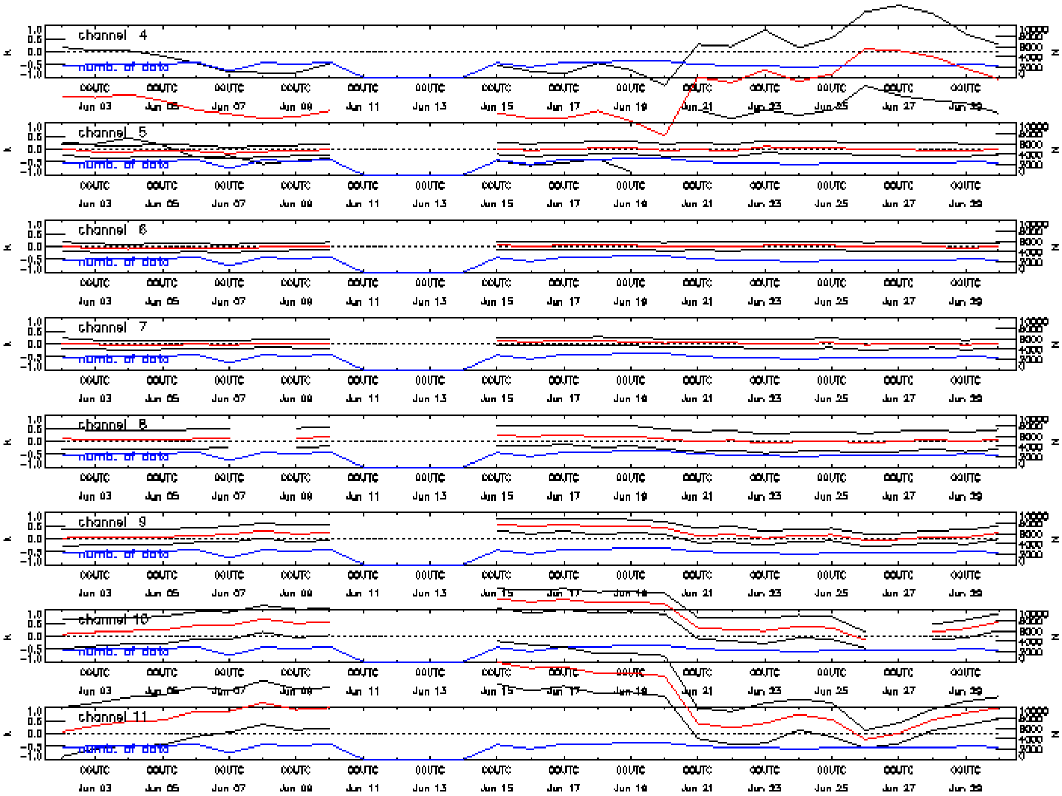

Figure 18: As Fig. 9 but for NOAA-16.